

Isothermal Adsorption and Desorption Properties of Marine Shales on Longmaxi Shale in South China

Taoyue Chang*, Yuanli Shu, Yue Ma,
Xinyi Xu, Yue Niu

College of Science, China University of Petroleum, Beijing, China

Email: *yuect@cup.edu.cn

How to cite this paper: Chang, T.Y., Shu, Y.L., Ma, Y., Xu, X.Y. and Niu, Y. (2017) Isothermal Adsorption and Desorption Properties of Marine Shales on Longmaxi Shale in South China. *Open Journal of Geology*, 7, 1819-1835.

<https://doi.org/10.4236/ojg.2017.712122>

Received: November 15, 2017

Accepted: December 26, 2017

Published: December 29, 2017

Copyright © 2017 by authors and Scientific Research Publishing Inc. This work is licensed under the Creative Commons Attribution International License (CC BY 4.0).

<http://creativecommons.org/licenses/by/4.0/>



Open Access

Abstract

The investigation of adsorption and desorption properties of shale are important for estimating reserves and exploitation. The shale samples used in this paper were from the marine shale on Longmaxi shale in Sichuan and Hubei province, China. A series of analyses, such as organic carbon content test, vitrinite reflectance test, rock pyrolysis, X-ray diffraction, and N₂/CO₂ adsorption were performed. Gravimetric method with magnetic suspension balance was used to conduct isothermal adsorption and desorption experiments. The Langmuir, Freundlich, Langmuir-Freundlich, D-R, semi-pore, and Toth equations were used to fit the isothermal adsorption and desorption curves. And adsorption potential theory was used to explain the adsorption and desorption process. According to the results, the shale samples have a high level of organic carbon content with the same organic matter type II₁ and high degree of maturation. The volume of adsorption increases rapidly and slows down to stable with the pressure increasing. Desorption is the inverse process of adsorption and 10 MPa - 0.5 MPa is the main period of shale gas desorption. The fitting results show that three-parameter isotherm equations are better than the two-parameter ones. The adsorption temperature has a great influence on adsorption volume, little effect on potential energy. Adsorption potential varies under different TOC to affect adsorption properties. Moreover, a large adsorption potential means that the gas molecule is easy to adsorb but difficult to desorb.

Keywords

Shale Gas, Isothermal Adsorption and Desorption, Gravimetric Method, Adsorption Potential

1. Introduction

Shale gas is an unconventional energy resource. The most remarkable difference between shale and conventional natural gas reservoirs is the difficulty in migrating shale gas [1]. Shale gas resources are widely distributed worldwide and the total amount of shale reserves is approximately $456.23 \times 10^{12} \text{ m}^3$. The prospect of exploiting this reservoir is favorable. North America was the first region to utilize shale gas reservoirs successfully with an annual production of shale gas reaching $1500 \times 10^8 \text{ m}^3$ until 2010 (Dong *et al.*, 2011; Zhang, 2011; EIA, May 5, 2011, April 5, 2011, December 16, 2011). Shale gas exploration and development in China is much later than in North America; nevertheless, China remains leading compared to other countries [2] [3] [4] [5]. Shale gas reservoirs in China mainly distribute in petroliferous basins, such as Sichuan, Ordos, Bohai Bay, Songliao, Jiangnan, Turpan-Hami, Tarim, and Jungga basins.

Shale gas exists in adsorbed, free, and dissolved state [6]. In the three states of shale gas, adsorption is the main state, and statistical results show that shale gas in adsorption state is 20% - 80% of the total shale gas reservoirs [7] [8] [9] [10]. Free gas comes out initially in the early exploitation period [11], the shale gas in adsorption state begins to emerge subsequently, because the pressure of shale gas reservoir decreases after the free gas materializes. Thus, studying the properties of the adsorption and desorption of shale are important for exploiting shale gas reservoirs. Many researchers [12] [13] [14] have done a lot of work on methane adsorption on shales. These existing experiments results almost were carried out by the method of the volumetric method, but few were by the methods of gravimetric method.

Adsorption is the process of molecule accumulation on the surface of shale as a consequence of surface energy minimization [14]. The adsorption process is generally identified as physisorption due to van der Waals forces and can be described by the potential theory [15] [16]. Besides, some researchers have recently studied how shale geological characteristics affect the adsorption capacity, and pressure and temperature regimes [14] [15] [17] [18].

In this study, shale samples were selected in some representative areas such as Yibin and Luzhou regions in Sichuan Province [19], Jingmen region in Hubei Province. A series of analyses, such as organic carbon content test, vitrinite reflectance test, rock pyrolysis, X-ray diffraction, and N_2/CO_2 adsorption were performed. Gravimetric method with magnetic suspension balance was used to conduct isothermal adsorption and desorption experiments. Some equations were used to fit the isothermal adsorption and desorption curves, respectively. Adsorption potential theory was used to explain the adsorption and desorption process.

2. Experimental Methods

2.1. Samples and Preparation

All the organic-rich shale samples were black mud shales of the lower Silurian

Longmaxi Formation widely developed in the Upper Yangtze Platform, south China. JING-1, JING-2, and JING-3 were from Jingmen region, Hubei Province; YS106 and YS109 were from Yibin region, Sichuan Province and YANG102 was from Luzhou region, Sichuan Province. Prior to measurement, 100 g of each sample was ground into powder of 60 - 80 mesh size. These powder samples were prepared for analysis of total organic carbon (TOC), rock pyrolysis, vitrinite reflectance test, X-ray diffraction (XRD), high pressure mercury test and N₂/CO₂ adsorption.

2.2. TOC, Rock Pyrolysis and Vitrinite Reflectance

WR-112 Laboratory Equipment Corporation (LECO) carbon analyzer of LECO Company, America was used to conduct the organic carbon analysis. The size of the sample particle is less than 0.2 mm. Iron and tungsten were added into the sample particle to aid combustion.

External standard analysis of the OGE workstation was used to conduct the continuous rock pyrolysis test, in which the first step was to heat to 300°C and then to 500°C.

UMSP-50 micro spectrophotometer was used to test vitrinite reflectance. The test conditions were temperature under 26°C, a wavelength of 546 nm ± 5 nm (green), and ×25 to ×100 unstrained oil immersion objective. One hundred tungsten halogen lamps and electronic exchange regulator of 3 kVA were also used.

2.3. X-Ray Diffraction and N₂/CO₂ Adsorption

The mineral composition test was done using XRD under Cu-Kα radiation. Emission and scattering slits are both 1°, and the receiving slit is 0.3 mm. The operating voltage is 30 KV - 45 KV, and the electric current is 20 mA - 100 mA; the scanning speed is 2°/min, and the sampling step width is 0.02°.

The Quadrasorb evo of Quantachrome, American was used to test mesopores structure and part of masopores structure by N₂ adsorption method. Before the test, all the samples were constant temperature dried under 105°C and vacuum, the adsorption gas purity is 99.99% and the experimental temperature is 77.35 K.

The Autosorb-iQ of Quantachrome, American was used to test micropores structure by CO₂ adsorption method. After degassing treatment, all shale samples were tested under 273.15 K.

2.4. Methane Isothermal Adsorption and Desorption Experiment

The volumetric method is commonly used in isothermal adsorption experiments on CBM and shale gas [20] [21] [22]. The principle of volumetric method is to calculate the adsorption volume according to the change of pressure.

In this study, the method selected to conduct the isothermal adsorption and desorption experiments is the gravimetric method with magnetic suspension balance (MSB; **Figure 1**). The weight of the shale sample was balanced using a

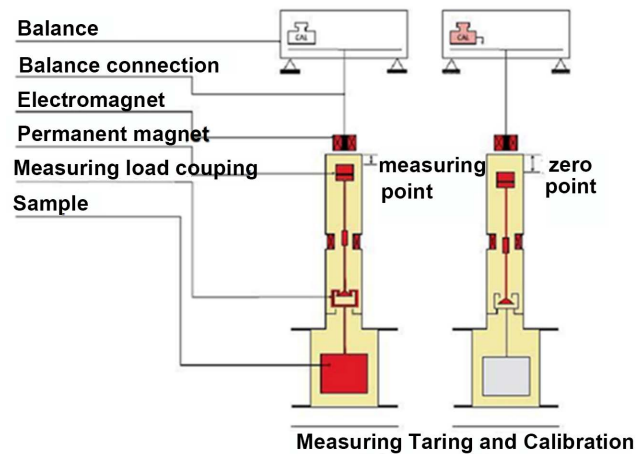


Figure 1. Work principles of MSB adsorption instrument.

non-contact suspending coupling mechanism. The balance has zero point and measuring point, and the two states automatically switch regularly to remove the inherent negative effects from zero drift effectively (reaching 0.00001 g accuracy). This design can achieve high precision measurement. The experiment process includes blank test, sample pretreatment, buoyance test, isothermal adsorption test, isothermal desorption test and data treating. Blank test tested without any sample in container and sample pretreatment avoided the influence from water and other gases aim to decrease the error. Shale samples were pretreated under 105°C and vacuumed before the isothermal adsorption experiment. The buoyance test was tested with helium to calibrate the buoyance of samples and container suffered after the pretreatment, which can calculate the adsorption volume accurately.

The adsorbed gas is 99.8% pure methane, and the experiment temperature is 30°C, and the shale samples were pulverized to 0.18 mm. The selected pressure points were 0 MPa, 0.5 MPa, 1 MPa, 2 MPa, 3 MPa, 4 MPa, 6 MPa, 10 MPa, 15 MPa, 20 MPa, 25 MPa, 30 MPa, and 33 MPa, respectively.

Desorption experiments were conducted under the same conditions as the adsorption experiments, except for the pressure setting. The selected pressure points for desorption were 33 MPa, 30 MPa, 25 MPa, 20 MPa, 15 MPa, 10 MPa, 6 MPa, 4 MPa, 3 MPa, 2 MPa, 1 MPa, 0.5 MPa, and 0 MPa, respectively.

3. Experimental Results

3.1. Geological Parameters Analysis Results

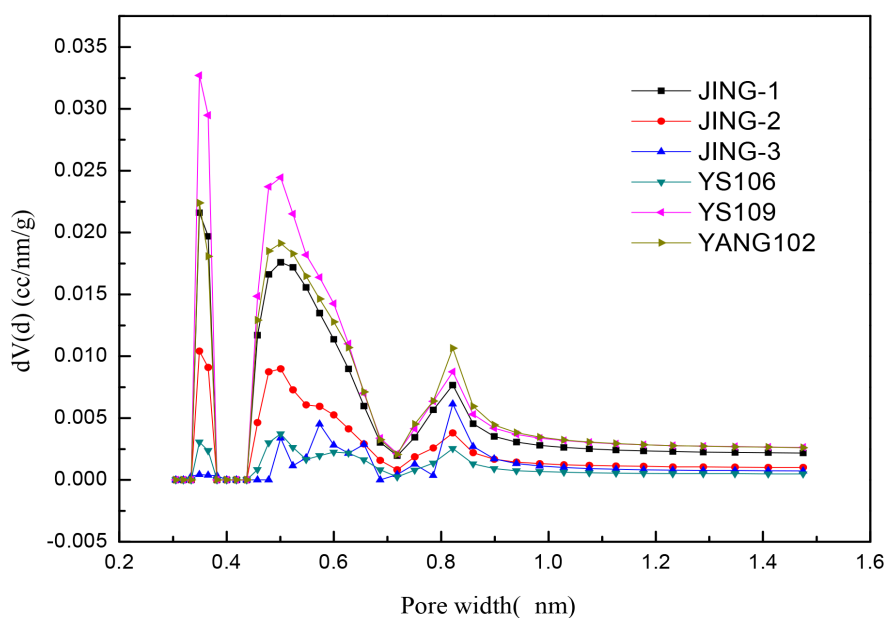
Table 1 shows that organic carbon content of the shale samples is 0.22% - 4.17% with an average of 1.92%. The organic matter type III indicates the high degree of organic matter maturity. The results of vitrinite reflectance are 1.92%-2.45% with an average of 2.11%, also indicating the high degree of organic matter maturity. Clay mineral content is 29.9% - 53.5% with an average of 42.0%. **Table 2** show the low temperature N₂ adsorption and CO₂ adsorption results, **Figure 2**

Table 1. Properties of shale samples.

Sample	Layer Formation	TOC%	Organic matter type	Vitrinite reflectance%	Clay mineral content%
JING-1	Longmaxi	4.17	II1	1.99	29.9
JING-2	Longmaxi	1.02	II1	2.07	44.2
JING-3	Longmaxi	0.43	II1	1.92	53.5
YS106	Qiongzhusi	0.22	II1	2.45	39.6
YS109	Longmaxi	2.55	II1	2.14	45.1
YANG102	Longmaxi	3.54	II1	2.07	39.9

Table 2. Pore construction of shale samples.

Sample	Pore Volume (cm ³ /g)			Specific surface area (m ² /g)	
	BJH		DFT	Micropores	Mesopores
	Adsorption	Desorption			
JING-1	0.005	0.005	0.004	19.71	8.39
JING-2	0.010	0.012	0.014	8.99	2.85
JING-3	0.008	0.008	0.035	3.77	4.03
YS106-1	0.003	0.004	0.002	3.48	1.22
YS109-1	0.012	0.014	0.013	15.46	2.17
YANG102	0.017	0.020	0.191	21.75	3.08

**Figure 2.** Distribution of micropores of shale samples.

and **Figure 3** respectively represent the pore size distribution micropores and mesopores. The pore volume of BJH method ranged from 0.003 cm³/g - 0.017 cm³/g, DFT method ranged from 0.002 cm³/g - 0.191 cm³/g. BJH method is used

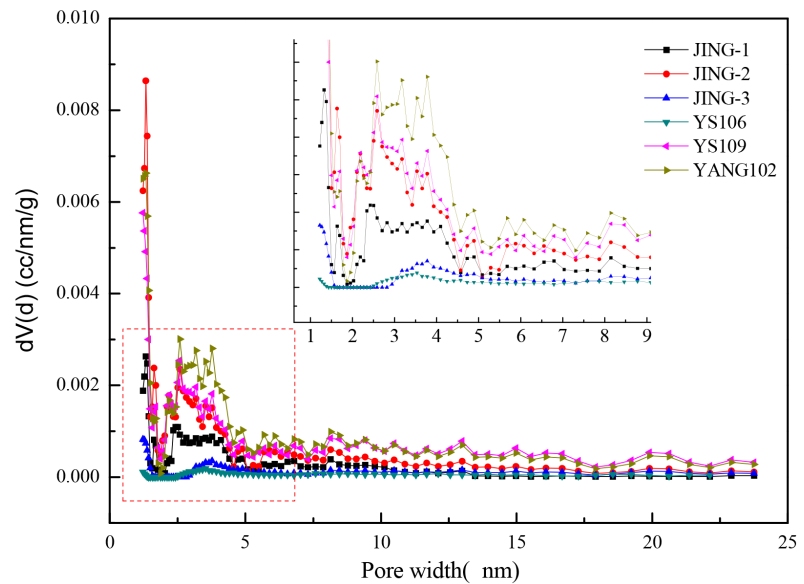


Figure 3. Distribution of mesopores of shale samples.

for calculate mesopore and a part of macropore. DFT method is used for calculate micropore and mesopore. Combining with the results in **Table 2**, **Figure 2** and **Figure 3**, it is shown that both method are similarity and the result of pore width is small. Therefore micropores developed well in the shale samples. The specific surface area of micropores ranged from $3.77 \text{ m}^2/\text{g}$ - $21.75 \text{ m}^2/\text{g}$ is larger than mesopores ranged from $1.22 \text{ m}^2/\text{g}$ - $8.39 \text{ m}^2/\text{g}$ in shale samples. Micropores controlled the adsorption process and had larger specific surface area, thus it was benefit to adsorb shale gas.

3.2. Results of Isothermal Adsorption and Desorption

MSB was used for the isotherm adsorption experiments. The results are listed in **Figure 4**, which shows that the adsorption volume increases rapidly at 0 MPa - 10 MPa. Micropores play a major role in the adsorption process, and the potential field of adjacent hole walls overlap. The adsorbed energy of the gas molecules is high; thus, the adsorption volume of the micropore filling is large [8]. The adsorption volume increases gradually at 10 MPa - 25 MPa, where in the mesopores begin to assume a major role. The specific surface and gravity of the wall of the hole is smaller than micropore, thus, adsorption velocity becomes slow. The adsorption volume nearly remained unchanged after 25 MPa; microporous and mesoporous adsorptions all reached saturation. Macropores have a large diameter, and gas molecules exist freely in them. Thus, the volume of adsorbed gas molecules, as well as the adsorption volume, does not increase.

Desorption is the inverse process of adsorption. MSB is also used to conduct the desorption experiments. Desorption velocity, which is an important parameter of shale gas desorption, is the ratio of desorbed gas volume to time [23] [24] [25]. The expression is

$$v = V/t \quad (1)$$

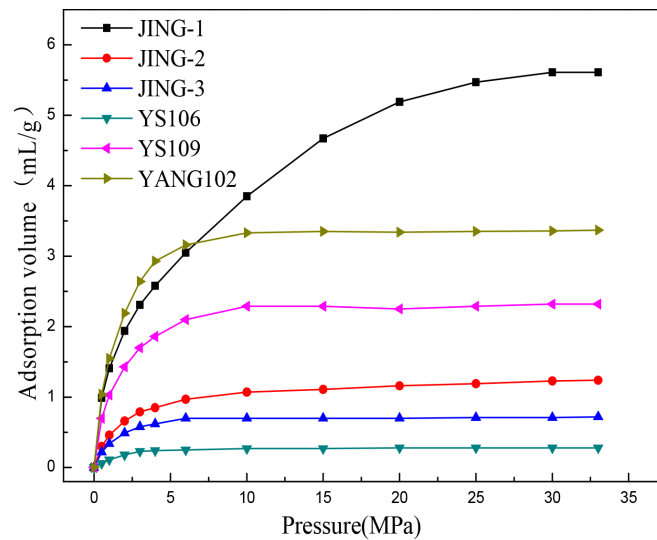


Figure 4. Isothermal adsorption curves of the shale samples at the same temperature.

where v represents the desorption rate ($\text{mL/g}\cdot\text{h}^{-1}$), V represents the desorption volume (mL/g), and t represents the time interval for desorption balance (h). The curves of isothermal desorption and desorption velocity are shown in **Figure 5**. **Figure 6** shows that when the pressure is high (33 MPa - 10 MPa), desorption velocity is small and remains at a relatively stable level. Desorption rate rises rapidly when pressure falls to 10 MPa, indicating that 10 MPa - 0.5 MPa is the main period of shale gas desorption.

3.3. Isothermal Adsorption and Desorption Fitting

Langmuir, Freundlich, Langmuir-Freundlich, D-R, and Toth equations are commonly used for isotherm adsorption to fit the adsorption curves [26] [27]. In addition, semi-pore equation is also used in this study to select out the best equation among the ones stated above. The equations are listed in **Table 3** [13] [28] [29] [30] [31].

V_L and V_0 are the saturated adsorption capacity (mL/g); P_L represents the Langmuir pressure (MPa); K represents the empirical constant; x represents the constant, $x < 1$; m is the heterogeneity parameter of adsorbent, $m \leq 1$; $b = 1/P_L$; D is the constant of the adsorbent; P_S denotes the saturated vapor pressure (MPa); α represent the parameters relative to the adsorbent or adsorbate property. k is the constant of inhomogeneity of adsorbent. **Table 3** shows that the Langmuir, Freundlich, and D-R equations comprise two parameters, whereas Langmuir-Freundlich, semi-pore, and Toth equations have three. Among these equations, Langmuir is the simplest and considers the monolayer adsorption on the adsorbent surface in the adsorption process. D-R equation is based on the micropore filling theory and is more suitable for microporous solids. The semi-pore equation, which can also be used in the study of shale gas, is proposed in the CBM research, and is based on the characteristics of irregular and porous

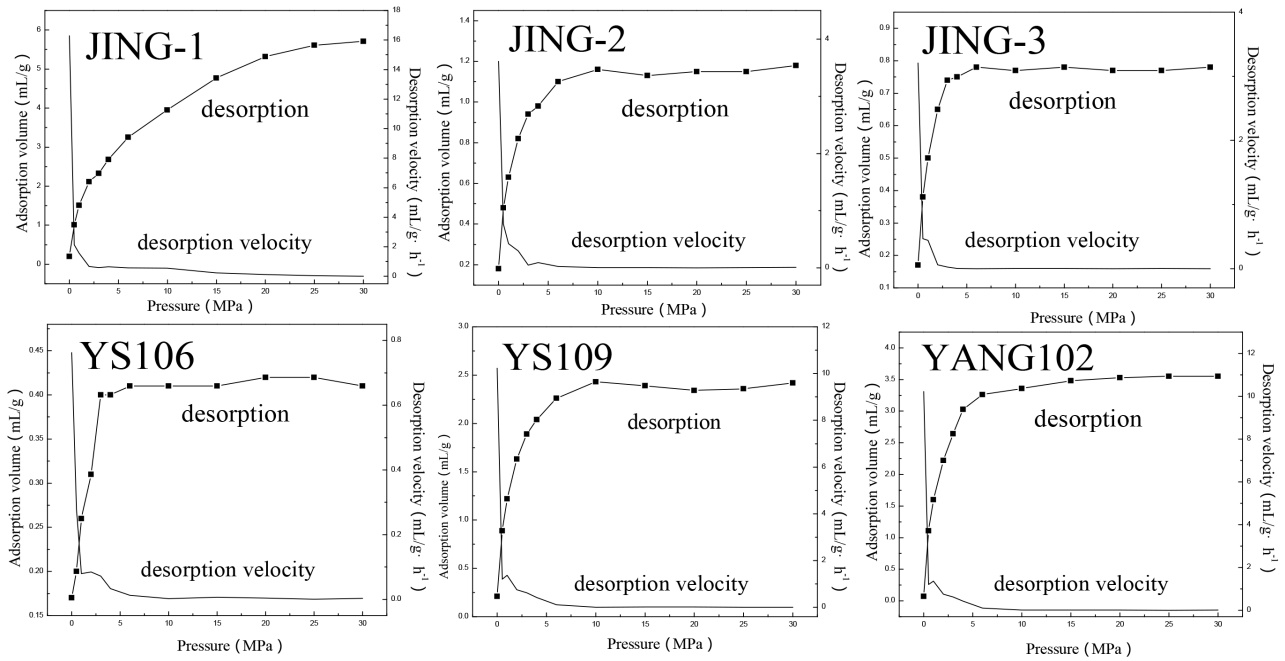


Figure 5. Curves of isothermal desorption volume and desorption velocity.

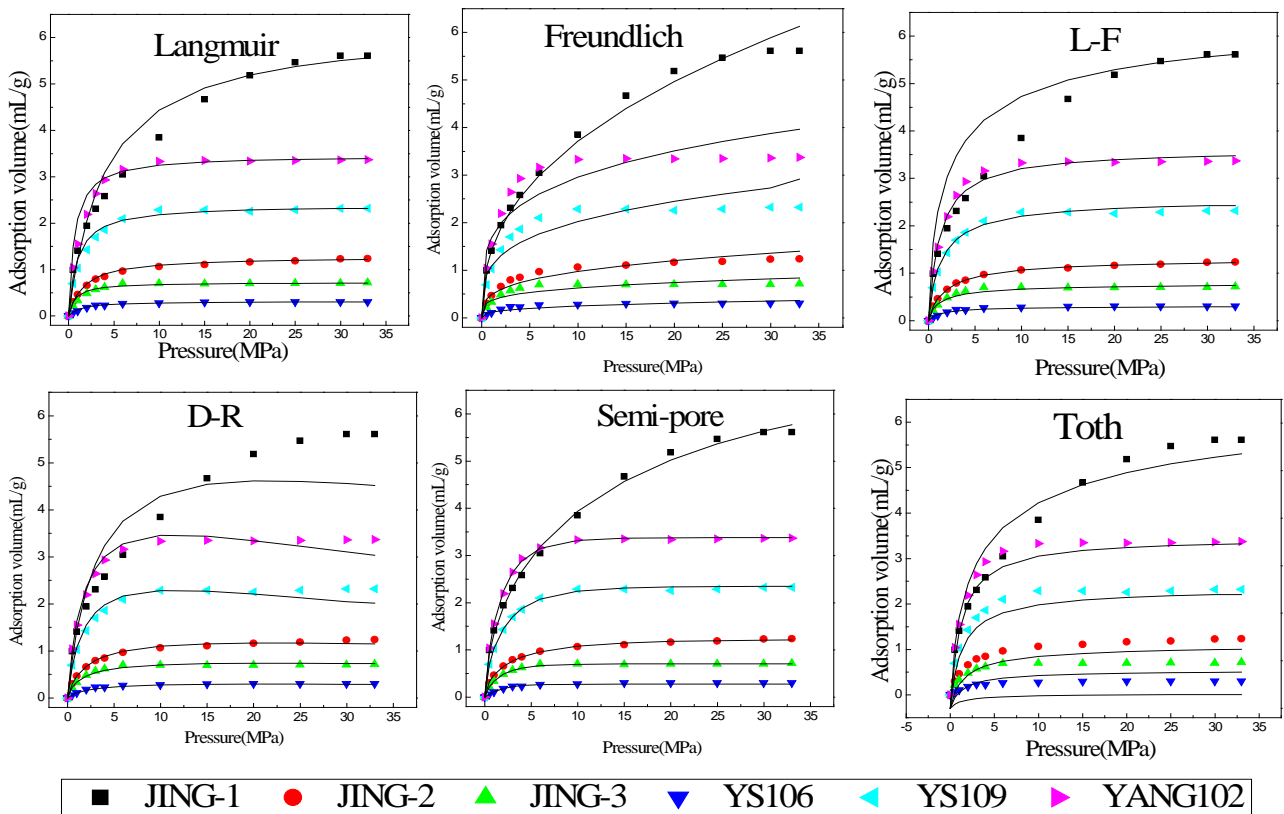


Figure 6. The curves of isothermal adsorption and fitting results of the isothermal equations.

pore structure. Freundlich, Langmuir-Freundlich, and Toth equations are either empirical or semi-empirical. Fitting results of these equations are shown in **Figure 6** and **Table 4**.

Table 3. Isothermal adsorption equations.

Isotherm model	Parameters	Equation
Langmuir	V_L, P_L	$V = \frac{V_L p}{P_L + p}$
Freundlich	K, x	$V = Kp^x$
Langmuir-Freundlich	V_L, m, b	$V = \frac{V_L (bp)^m}{1 + (bp)^m}$
D-R	D, V_0	$V = V_0 \exp[-D \ln^2 (P_s/P)]$
Semi-pore	V_L, b, α	$V = V_L [1 - \exp(-bp^\alpha)]$
Toth	V_L, b, k	$V = \frac{V_L bp}{[1 + (bp)^k]^{1/k}}$

Table 4. Comparison of V_L of adsorption and desorption (mL/g).

Sample	Langmuir equation		Langmuir-Freundlich equation		D-R equation		Semi-pore equation		Toth equation	
	Ads	Des	Ads	Des	Ads	Des	Ads	Des	Ads	Des
JING-1	6.25	6.32	6.48	6.81	4.62	4.75	7.33	7.38	7.04	7.56
JING-2	1.28	1.28	1.33	1.40	1.17	1.18	1.22	1.23	1.36	1.38
JING-3	0.72	0.78	0.80	0.84	0.73	0.80	0.70	0.79	0.80	0.81
YS106	0.32	0.42	0.31	0.43	0.30	0.43	0.27	0.42	0.31	0.43
YS109	2.39	2.46	2.58	2.63	2.29	2.44	2.39	2.46	2.58	2.63
YANG102	3.46	3.68	3.61	3.99	3.47	3.60	3.46	3.68	3.61	3.99

Note: Ads = adsorption; Des = desorption.

As shown in **Figure 6**, the results of all the isothermal equations fit well. Langmuir, semi-pore, and Toth equations are better than Freundlich and D-R equations. Relative errors were calculated to determine the best fitting equation for isothermal adsorption process, as shown in **Figure 7**.

Figure 7 shows that the best equation for fitting in the isothermal adsorption process is the semi-pore equation, which has a relative fitting error of under 5%. Fitting results of the three-parameter equations are better than the two-parameter ones, because there a parameter relative to non-uniformity of the shale surface exists in the three-parameter equations. The presence of the third parameter reduces the error more effectively. The Langmuir equation is the most widely used equation because of its simple expression, physical meaning of its parameters, and good fitting results.

The Langmuir, Freundlich, Langmuir-Freundlich, D-R, Toth, and semi-pore equations were also used to fit the desorption curves. V_L of desorption fitting is compared with that of adsorption fitting. The fitting results of desorption and comparison results are shown in **Figure 8** and **Table 4**, respectively.

Desorption fitting results are similar to adsorption, with the Langmuir-Freundlich, semi-pore, and Toth equations as the best fitting equations. As shown in **Table 4**, the V_L of the desorption process is larger than that of the adsorption one, which is called desorption hysteresis. This result is probably due to

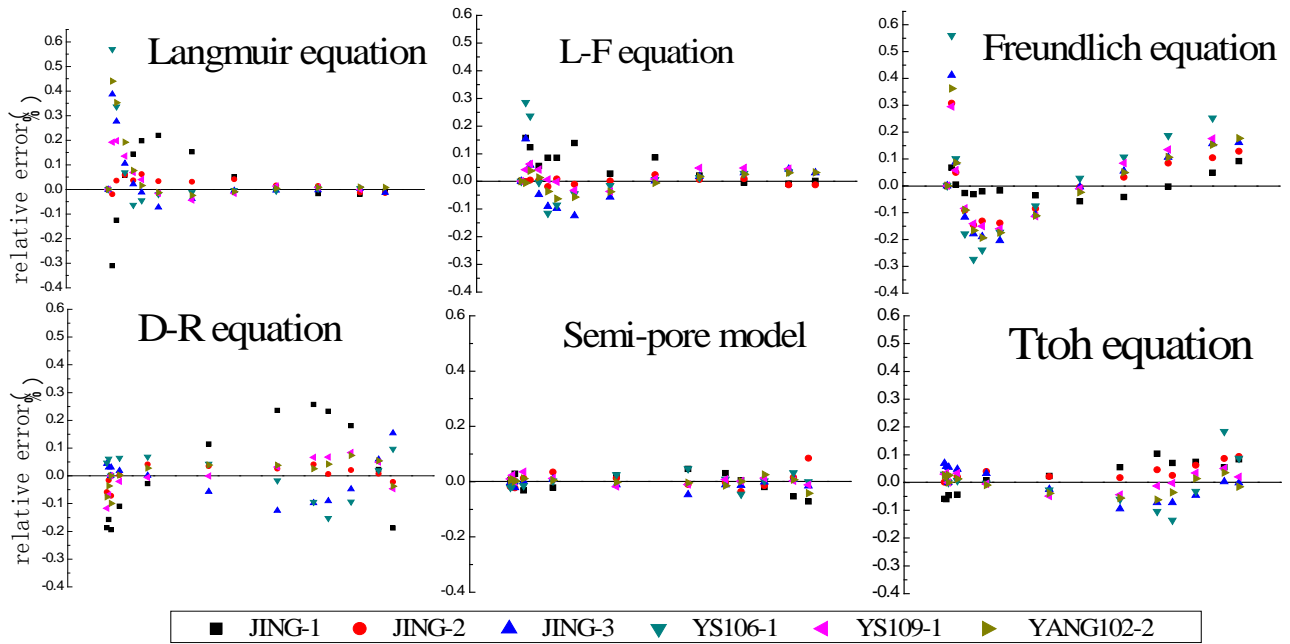


Figure 7. Fitting errors distribution of isothermal equations of adsorption.

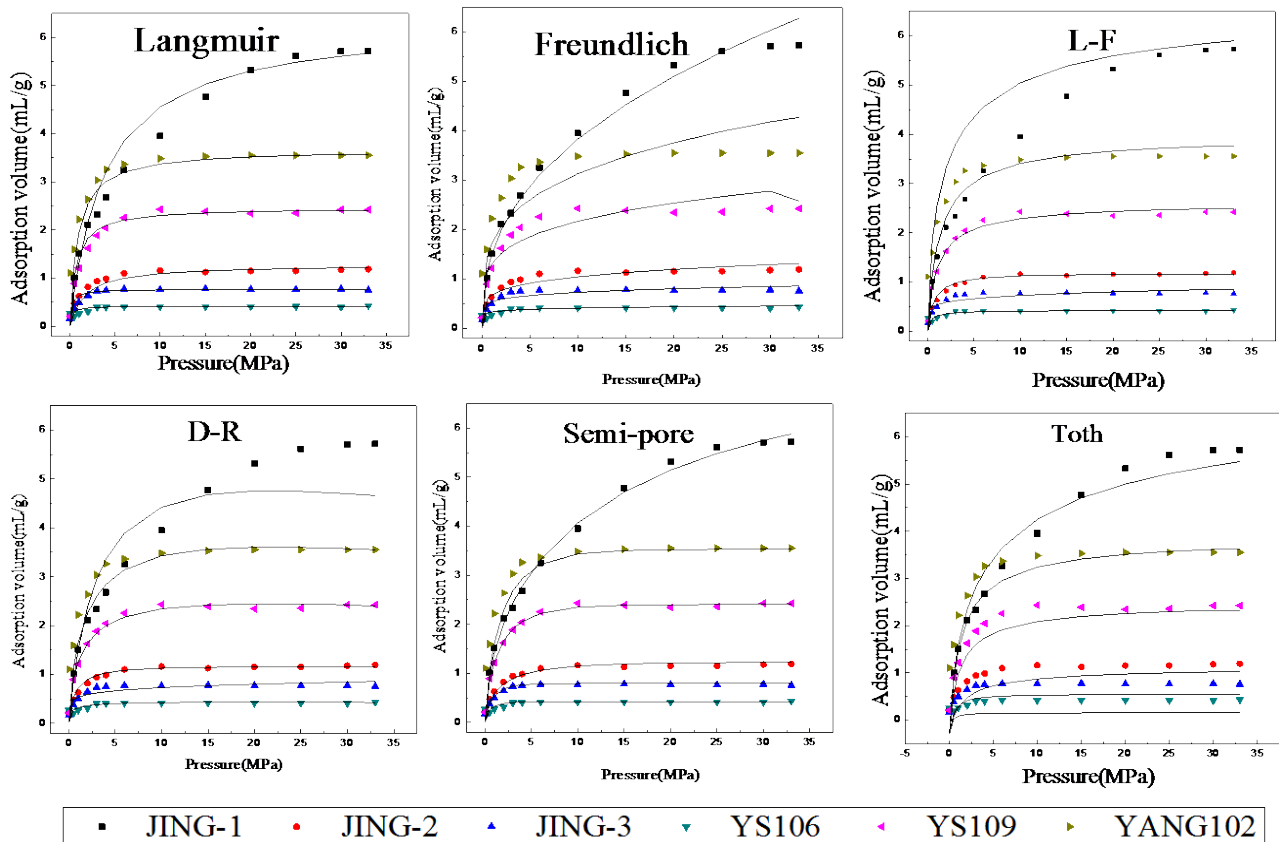


Figure 8. The curves of isothermal desorption and fitting results of the isothermal equations.

the capillary condensation in the pores of the shales or the changed pore structures during adsorption. The specific reasons need to be further studied.

4. Application of Adsorption Potential Theory

4.1. Adsorption Potential Theory

Adsorption potential theory is proposed by Polanyi for physical adsorption process, which was expressed as [32]

$$\varepsilon = \int_P^{P_s} V dP = \int_P^{P_s} \frac{RT}{P} dP = RT \ln(P_s/P) \quad (2)$$

where ε represents adsorption potential (J/mol), V is the gas volume of free state (cm^3/g), P_s is the saturated vapor pressure (MPa) when the temperature is T , P is the balance pressure (MPa), T is the temperature of experiment (K), and R is gas constant ($\text{J}/\text{mol}\cdot\text{K}^{-1}$).

When the experimental temperature is more than the critical temperature, the concept of saturation vapor pressure at above the critical temperature does not exist, that is to say, the saturation vapor pressure lose physical meaning. Thus, an experience formula established by Dubinin is used to calculate the virtual saturation vapor pressure P_v of methane in supercritical condition. The equation is showed as [33].

$$P_v = P_c \left[\frac{T}{T_c} \right]^2 \quad (3)$$

where P_c is supercritical pressure (MPa), and T_c is supercritical temperature (K). Adsorption potential becomes large with the decrease of distance between gas molecules and shale surface. Potential field direction is determined from the adsorption phase to bulk phase. Adsorption potential can be expressed as the distance by the adsorbate molecule from its site to zero point. The gas molecule is in free state when adsorption potential is negative and is in adsorption state when adsorption potential is positive.

The adsorption potential theory was used to explain the shale isotherm factors, and it was also used to explain desorption process and estimate the degree of difficulty of different shale samples.

4.2. Adsorption Process

Saturated vapor pressures of methane at 30°C, 50°C, 70°C, and 90°C were 11.68 MPa, 13.28 MPa, 14.99 MPa, and 16.80 MPa, respectively. The adsorption potential and adsorption results of JING-1 at different temperatures are shown in **Figure 9**.

Figure 9 shows that the adsorption potential becomes larger with the increase of temperature at the same pressure. Thus, the attraction from adsorbent surface becomes larger and more prone to adsorption. Meanwhile, the isothermal adsorption curve at 30°C is much higher than others. With temperature increasing, potential energy also increase when gas molecules move to the solid surface of shale from bulk phase to adsorbed phase. In theory, the increase in temperature would benefit the adsorption. However, the thermal motion of gas molecules also rises up and plays a greater influence. Comparing with the relationship

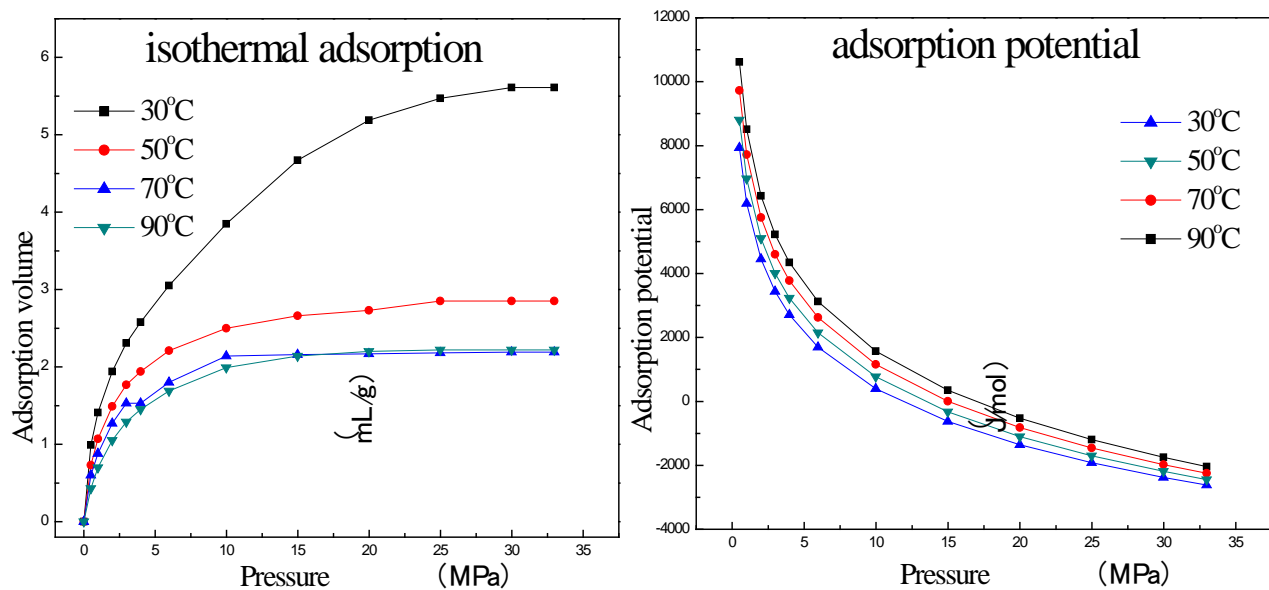


Figure 9. Curves of isothermal adsorption and adsorption potential of JING-1 at different temperatures.

among adsorption volume, temperature and potential energy, it is obvious that temperature has a great influence on adsorption volume, little effect on potential energy.

JING-1, JING-2, and JING-3 samples have different TOC. The adsorption potential of these samples, when the adsorption volumes are 0.20 mL/g, 0.30 mL/g, 0.50 mL/g, 0.60 mL/g, and 0.70 mL/g, respectively, are shown in **Figure 10**. As shown in **Figure 10**, the adsorption potential becomes larger with the increase of TOC when the adsorption volume is constant. A greater adsorption potential also means a greater attraction between adsorption surface and gas molecules. Thus, the adsorption capacity of JING-1 sample is best.

Figure 11 shows the results of adsorption of shale with and without moisture. The moisture sample was prepared according to the standards of the American Society for Testing and Materials [12]. The shale samples were placed into water for 2 h to 3 h, underwent vacuum suction, and then placed in a vacuum dryer (within supersaturated solution of potassium sulfate). The evacuation condition is 20 kPa, and the samples were weighted every 24 h until the weight of two adjacent samples is less than 2%.

The critical temperature of methane is -82.6°C , over this temperature the state is called supercritical state. When the experimental temperature is more than the critical temperature, the concept of saturation vapor pressure at above the critical temperature does not exist, that is to say, the saturation vapor pressure lose physical meaning. In this manuscript, the adsorption capacity is regarded as excess adsorption, and it is greater than absolute adsorption. As shown in **Figure 11**, the adsorption capacity of the moisturized sample is remarkably smaller than the dried sample, because the saturation vapor pressure of the mixed gas of methane and vapor is significantly smaller than pure methane.

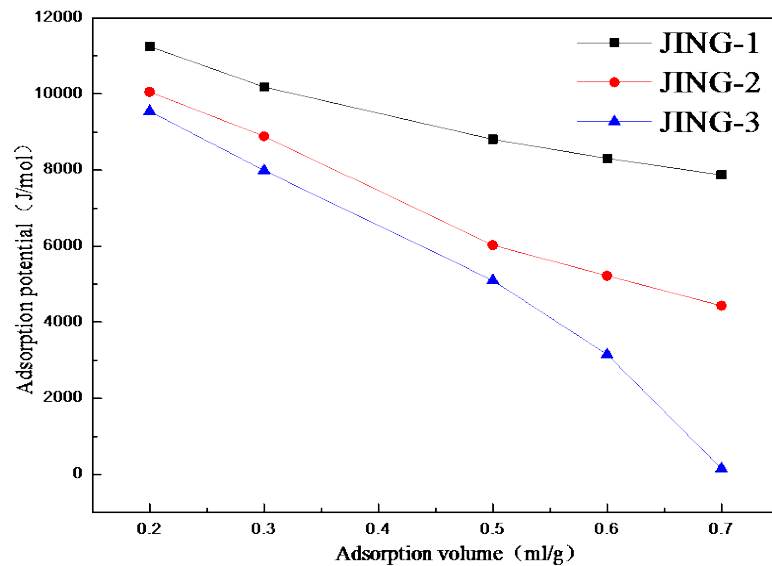


Figure 10. Adsorption potential of samples at different TOC at the same volume.

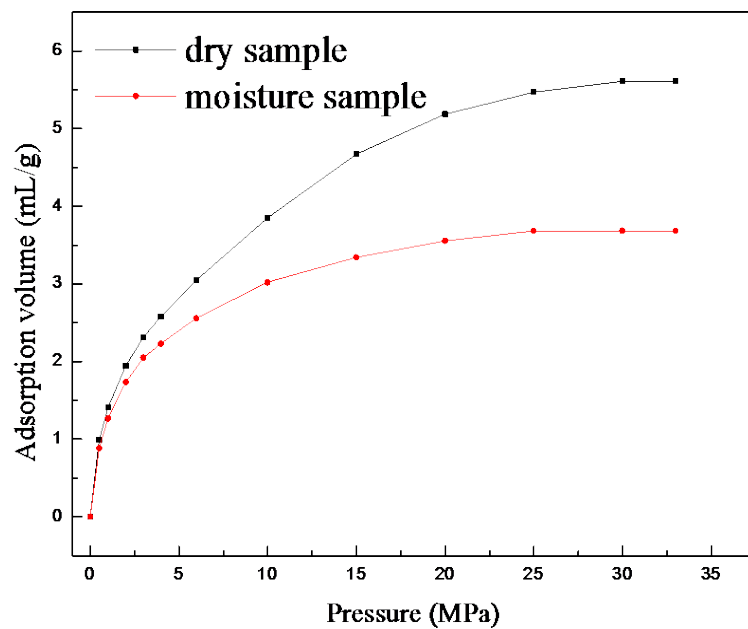


Figure 11. Curves of the JING-1 isothermal adsorption under different water conditions.

4.3. Desorption Process

The curves of adsorption potential and desorption velocity are shown in **Figure 12**. The adsorption potential curves have the same trend with desorption velocity curves. When pressure is high, the adsorption potential of gas molecules is negative and its existence state is free. Moreover, under this condition, slight desorption and small desorption velocity were present. When pressure dropped to 10 MPa, the adsorption potential of gas molecules began to become positive with an absorbed state. Thereafter, the adsorbed molecules started to escape; the volume

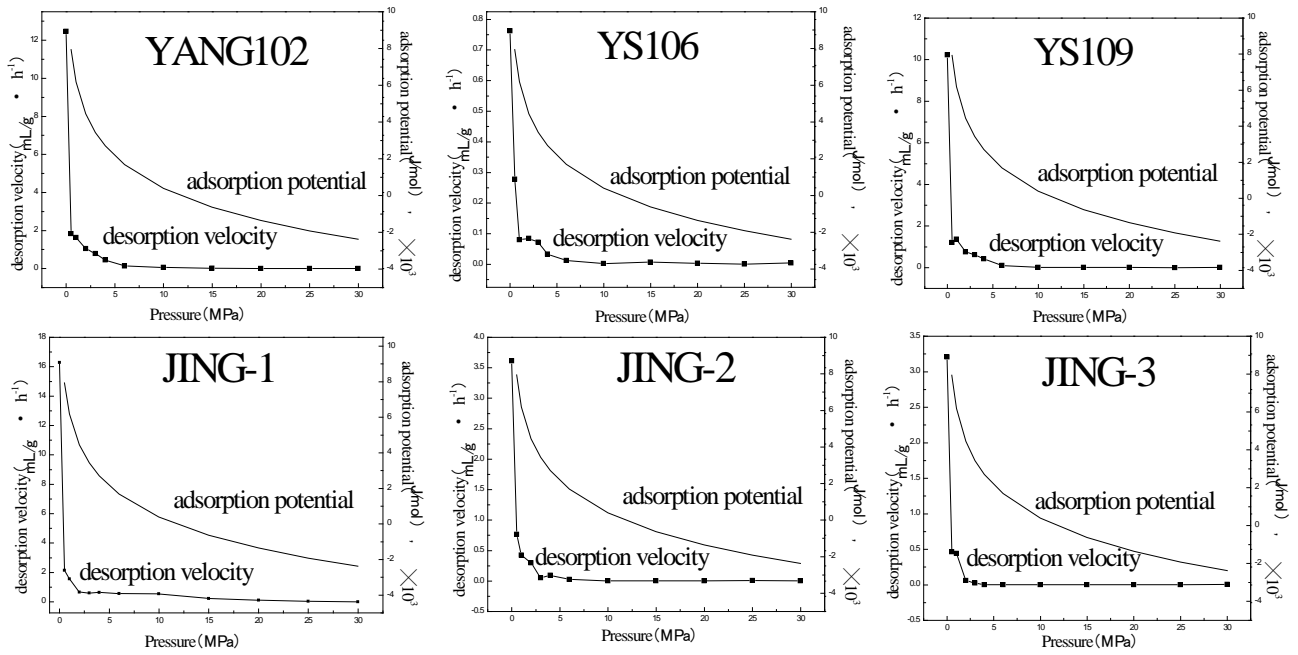


Figure 12. Curves of desorption velocity and adsorption potential.

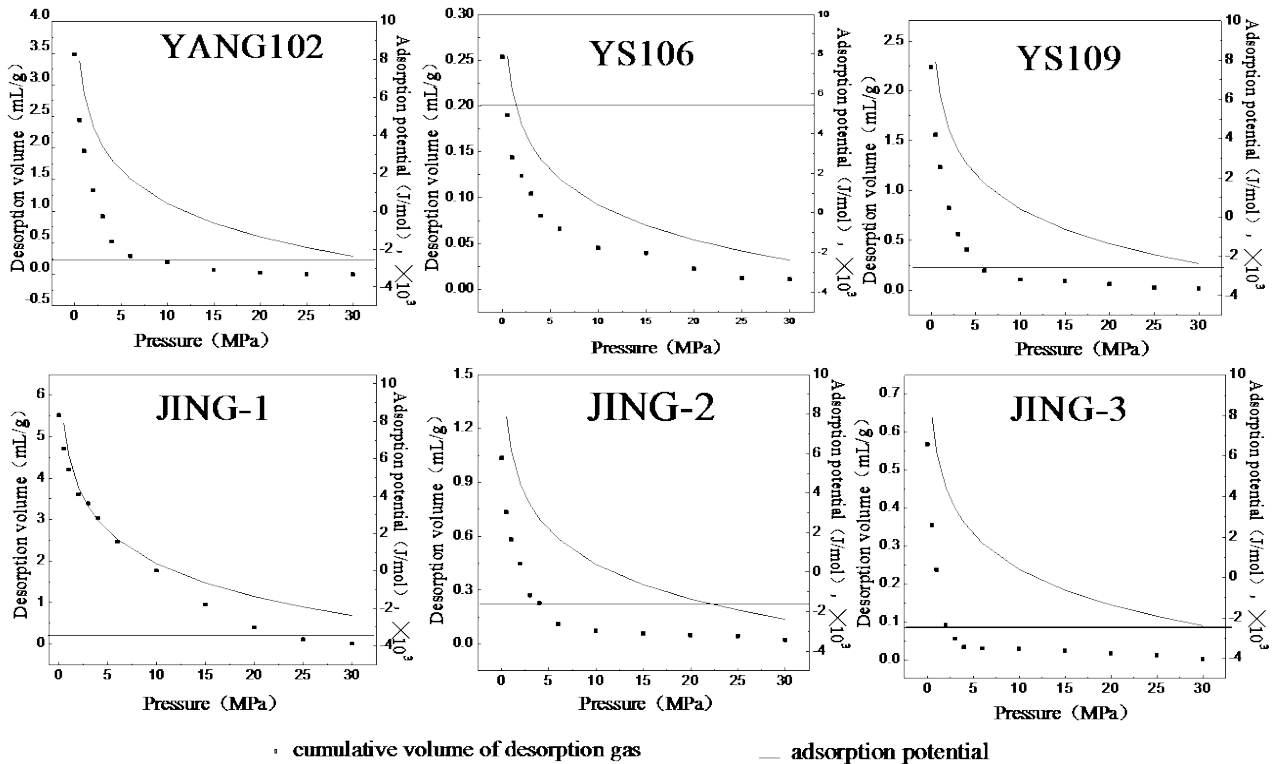


Figure 13. Relationship between cumulative desorption volume and adsorption potential.

of desorbed gas became high, and desorption velocity began to increase rapidly. The maximum slopes of adsorption potential curves emerge in the range from 10 MPa - 0.5 MPa, and desorption velocity also began to increase rapidly at the same time.

The relationship of cumulative volume of desorption gas and adsorption potential is shown in **Figure 13**. The horizontal line represents the cumulative volume of desorption gas, which is 0.20 mL/g. The relationship of adsorption potential is YS106 > JING-3 > JING-2 > YS109 > YANG102 > JING-1 when the cumulative adsorption is identical. Among the samples, JING-1 was most prone to desorption, and YS106 was the most difficult to desorbed.

5. Conclusions

1) According to the adsorption experiment results, the volume of adsorption increases rapidly at low pressure 0 MPa - 10 MPa, and slows down with the pressure rise. In the desorption process, desorption volume is relative hysteresis.

2) The adsorption equations were used to fit the isothermal adsorption and desorption curves. The results show that three-parameter equations fit better than the two-parameter ones.

3) Adsorption potential theory can be used to explain the adsorption and desorption process. The adsorption temperature has a great influence on adsorption volume, little effect on potential energy.

4) The conclusions discuss the adsorption characters of single component gas. The next study can focus on the competitive adsorption of binary component gas and optimum calculation method of adsorption volume.

Acknowledgements

This work was supported by the General Program of National Natural Science Fund of China (No. 41372152).

References

- [1] Zhang, L.Y., Li, Z. and Zhu, R.F. (2009) The Formation and Exploitation of Shale Gas. *Natural Gas Industry*, **1**, 124-128. (in Chinese)
- [2] Dong, D.Z., Zou, C.N., Li, J.Z., *et al.* (2011) Resource Potential, Exploration and Development Prospect of Shale Gas in the Whole World. *Geological Bulletin of China*, **30**, 324-336. (In Chinese)
- [3] Zhang, D.W. (2011) Main Solution Ways to Speed up Shale Gas Exploration and Development in China. *Natural Gas Industry*, **31**, 1-5. (In Chinese)
- [4] Zhang, H.X. (2010) Shale Gas: New Bright Point of the Exploration of the Global Oil-gas Resources. *Strategy & Policy Decision Research*, **25**, 406-410. (In Chinese)
- [5] Zou, C.N., Dong, D.Z., Wang, S.J., *et al.* (2010) Geological Characteristics, Formation Mechanism and Resource Potential of Shale Gas in China. *Petroleum Exploration and Development*, **37**, 641-653. [https://doi.org/10.1016/S1876-3804\(11\)60001-3](https://doi.org/10.1016/S1876-3804(11)60001-3)
- [6] Richard, M.P. (2007) Total Petroleum System Assessment of Undiscovered Resources in the Giant Barnett Shalecontinuous (Unconventional) Gas Accumulation, Fort Worth Basin, Texas. *AAPG Bulletin*, **91**, 551-578. <https://doi.org/10.1306/06200606007>
- [7] Zhang, H.Z. and He, Y.Q. (2010) Resource Potential and Development Status of Global Shale Gas. *Oil Forum*, **6**, 53-57. (In Chinese)
- [8] Curtis, J.B. (2002) Fractured Shale-Gas Systems. *AAPG Bulletin*, **86**, 1921-1938.

- [9] Ross, D.J. and Bustin, R.M. (2007) Shale Gas Potential of the Lower Jurassic Gordondale Member, Northeastern British Columbia, Canada. *Bulletin of Canadian Petroleum Geology*, **55**, 51-75. <https://doi.org/10.2113/gscpgbull.55.1.51>
- [10] Lu, X.C., Li, F.C. and Watson, A.T. (1995) Adsorption Measurements in Devonian Shales. *Fuel*, **74**, 599-603. [https://doi.org/10.1016/0016-2361\(95\)98364-K](https://doi.org/10.1016/0016-2361(95)98364-K)
- [11] Grieser, W.V., Shelley, R.F. and Soliman, M.Y. (2009) Predicting Production Outcome from Multi-Stage, Horizontal Barnett Completions. *SPE Production and Operations Symposium, Oklahoma: SPE*, 259-268.
- [12] Xie, Z.H. and Chen, S.J. (2007) Effect of Moisture and Temperature to CH₄ Adsorption of Coal. *Journal of University of Science and Technology Beijing*, **29**, 42-44. (In Chinese)
- [13] Xiong, W., Guo, W., Liu, H.L., *et al.* (2012) Shale Reservoirs Characteristics and Isothermal Adsorption Properties. *Natural Gas Industry*, **32**, 113-130. (In Chinese)
- [14] Zhang, Z.Y. and Yang, S.B. (2012) On the Adsorption and Desorption Trend of Shale Gas. *Journal of Experimental Mechanics*, **27**, 492-497. (In Chinese)
- [15] Ross, D.J. and Bustin, R.M. (2008) Characterizing the Shale Gas Resource Potential of Devonian-Mississippian Strata in the Western Canada Sedimentary Basin: Application of an Integrated Formation Evaluation. *AAPG Bulletin*, **92**, 87-125. <https://doi.org/10.1306/09040707048>
- [16] Bjoener, M.G., Shaouri, A.A. and Kontogeorgis, G.M. (2013) Potential Theory of Adsorption for Associating Mixtures: Possibilities and Limitations. *Industrial & Engineering Chemistry Research*, **52**, 2672-2684. <https://doi.org/10.1021/ie302144t>
- [17] Rexer, T.F., Benham, M.J., Aplin, A.C. and Thomas, K.M. (2013) Methane Adsorption on Shale under Simulated Geological Temperature and Pressure Conditions. *Energy Fuels*, **27**, 3099-3109. <https://doi.org/10.1021/ef400381y>
- [18] Tan, J., Weniger, P., Krooss, B., *et al.* (2014) Shale Gas Potential of the Major Marine Shale Formations on the Upper Yangtze Platform, South China. Part II: Methane Sorption Capacity. *Fuel*, **129**, 204-218. <https://doi.org/10.1016/j.fuel.2014.03.064>
- [19] Boling, P.U., Jiang, Y.L., *et al.* (2010) Reservoir-Forming Conditions and Favorable Exploration Zones of Shale Gas in Lower Silurian Longmaxi Formation of Sichuan Basin. *Acta Petrolei Sinica*, **31**, 225-230.
- [20] Xie, J.L., Guo, Y.Y. and Wu, S.Y. (2004) Study on Adsorption of Methane on Coal at Normal Temperature. *Journal of Taiyuan University of Technology*, **35**, 562-567. (In Chinese)
- [21] Guo, W., Hu, Z., Zhang, X., Yu, R. and Wang, L. (2017) Shale Gas Adsorption and Desorption Characteristics and Its Effects on Shale Permeability. *Energy Exploration & Exploitation*, **35**, 463-481. <https://doi.org/10.1177/0144598716684306>
- [22] Kondo, Ishikawa, T. and Abe, I. (2006) Adsorption Science. Chemical Industry Press, Beijing, 50 p. (In Chinese)
- [23] Peng, J.N., Fu, X.H., Shen, J. and Zhu, Y.W. (2005) Study of Desorption Characteristics of Coaled Methane in Panzhuang Mining Area. *Natural Gas Geoscience*, **16**, 766-770. (In Chinese)
- [24] Lane, H.S., Watson, A.T. and Lancaster, D.E. (1989) Identifying and Estimating Desorption from Devonian Shale Gas Production Data. *Pediatrics*, **35**, 22-28. <https://doi.org/10.2523/19794-MS>
- [25] Lane, H.S., Lancaster, D.E. and Watson, A.T. (1991) Characterizing the Role of Desorption in Gas Production from Devonian Shales. *Energy Sources*, **13**, 337-359. <https://doi.org/10.1080/00908319108908993>

-
- [26] Kong, D., Ning, Z., Yang, F., *et al.* (2013) The Characteristic of Adsorption on Shales and Influence Factor. *Petrochemical Industry Application*, **32**, 1-4. (In Chinese)
- [27] Zhao, T.Y., Ning, Z.F. and Zeng, Y. (2014) Comparative Analysis of Isothermal Adsorption Models for Shales and Coals. *Xinjiang Petroleum Geology*, **35**, 319-323. (In Chinese)
- [28] Yang, F., Ning, Z.F., Kong, D.T., *et al.* (2013) Comparison Analysis on Model of Methane Adsorption Isothermal in Shales. *Coal Science and Technology*, **41**, 86-89. (In Chinese)
- [29] Su, X.B., Chen, R., Lin, X.Y., *et al.* (2008) Application of Adsorption Potential Theory in the Fractionation of Coalbed Gas during the Process of Adsorption/Desorption. *Acta Geologica Sinica*, **82**, 1382-1388. (In Chinese)
- [30] Yu, H.G., Fan, W.T., Sun, M.Y., *et al.* (2004) Study on Fitting Models for Methane Isotherms Adsorption of Coals. *Journal of China Coal Society*, **29**, 463-467. (In Chinese)
- [31] Ma, D.M. (2008) Research on the Adsorption and Desorption Mechanism of Coalbed Methane. Thesis, Xi'an University of Science and Technology, Xi'an, 65-66. (In Chinese)
- [32] Liu, B.A., Dong, Y.H. and Liu, X.F. (1993) Briefly Deduced of Polanyi Adsorption Potential Theory. *Journal of Shandong Institute of Building Material*, **13**, 105-108. (In Chinese)
- [33] Dubinin, M.M. (1960) The Potential Theory of Adsorption of Gases and Vapors for Adsorbents with Energetically Nonuniform Surfaces. *Chemical Reviews*, **60**, 235-241. <https://doi.org/10.1021/cr60204a006>